Wind and Structures, *Vol. 25, No. 5 (2017) 475-492*
DOI: https://doi.org/10.12989/was.2017.25.5.475

Aerodynamic coefficients of inclined and yawed circular cylinders with different surface configurations

Siyuan Lin[1,2a], Mingshui Li[*1,2] and Haili Liao[1,2b]

[1]*Research Centre for Wind Engineering, Southwest Jiaotong University, Chengdu, Sichuan 610031, China*
[2]*Key Laboratory for Wind Engineering of Sichuan Province, Chengdu, Sichuan 610031, China*

(Received February 20, 2017, Revised September 23, 2017, Accepted November 7, 2017)

Abstract. Inclined and yawed circular cylinder is an essential element in the widespread range of structures. As one of the applications, cables on bridges were reported to have the possibility of suffering a kind of large amplitude vibration called dry galloping. In order to have a detailed understanding of the aerodynamics related to dry galloping, this study carried out a set of wind tunnel tests for the inclined and yawed circular cylinders. The aerodynamic coefficients of circular cylinders with three surface configurations, including smooth, dimpled pattern and helical fillet are tested using the force balance under a wide range of inclination and yaw angles in the wind tunnel. The Reynolds number ranges from 2×10^5 to 7×10^5 during the test. The influence of turbulence intensity on the drag and lift coefficients is corrected. The effects of inclination angle yaw angle and surface configurations on the aerodynamic coefficients are discussed. Adopting the existed the quasi-steady model, the nondimensional aerodynamic damping parameters for the cylinders with three kinds of surface configurations are evaluated. It is found that surface with helical fillet or dimpled pattern have the potential to suppress the dry galloping, while the latter one is more effective.

Keywords: inclined and yawed circular cylinder; surface configuration; Reynolds number; drag coefficient; lift coefficient; nondimensional aerodynamic damping parameter

1. Introduction

Circular cylinders have long been used as an important element in various kinds of structures, including cables, pipelines, towers, chimneys, lattice towers, missiles, etc. As a typical inclined and yawed circular cylinder, widespread applications of cables emerged with the construction of cable-stayed bridges around the world in the past several decades. However, stay cables would often face large amplitude vibration due to their flexibility and low damping. It was observed that a significant correlation between the occurrences of wind and rain exists, thus the term of rain-wind-induced vibration (RWIV) was adopted. Apart from RWIV, some field observations (Matsumoto, Yagi *et al.* 2005, Boujard and Grillaud 2007) and a few experimental studies (Cheng *et al.* 2003, Jakobsen *et al.* 2012) show that inclined and yawed cables would also suffer

∗Corresponding author, Professor, E-mail: lms_rcwe@126.com
[a] Ph.D. Student, E-mail: linsiyuan01@gmail.com
[b] Professor, E-mail: hlliao@swjtu.edu.cn

http://www.techno-press.org/?journal=was&subpage=8 ISSN: 1226-6116 (Print), 1598-6225 (Online)

wind-induced instability without the existence of rain, of which the phenomenon is termed as "dry galloping".

For the rain-wind-induced problem, extensive experimental and theoretical studies on inclined cables have been performed in sufficient detail (Acampora *et al*. 2014, Jing *et al.* 2017). The proposed countermeasures, including changing the surface configuration or increasing the damping with TMD on stay cables turn out to be effective. However, the mechanism inherent in galloping of dry inclined and yawed cables is rather complex.

To investigate the characteristics of dry galloping, (Cheng *et al.* 2003) first designed a special test rig for the dynamic test of the inclined cables in an open circuit wind tunnel at the National Research Council Canada (NRC). Divergent and limited amplitude vibrations of dry, non-iced smooth cable were observed in specific combinations of inclination and yawed angle in the critical Reynolds number range. In a further experimental study, the pressure distribution and vibration response were measured simultaneously for the cables in the dynamic test (Jakobsen *et al*. 2012, Nikitas *et al.* 2012).

Besides the direct experimental study, flow-induced forces on yawed and inclined circular cylinders were modeled based on the quasi-steady approach (Carassale *et al*. 2005). A nondimensional aerodynamic damping parameter considering the effects of Reynolds number, the angle between the wind velocity and the cable axis and the orientation of the vibration plane was proposed to evaluate the instability of dry galloping(Macdonald and Larose 2006). The galloping instability predicted by the above theoretical model and criterion fits well with the dynamic test results. A three-dimensional aeroelastic model has been also proposed to study the effect of unsteady wind condition on the wind-induced response of bridge cables recently(Raeesi *et al.* 2016).

However, the above mentioned force model, nondimensional aerodynamic damping parameter and the three-dimensional aeroelastic model are all calculated based on the drag and lift coefficients measured in wind tunnel tests. Larose measured the pressure distribution of a stationary cable in the wind tunnel and calculated the aerostatic coefficients of the inclined and yawed circular cylinders(Larose *et al*. 2003). The pressure measuring method can get the pressure distribution around the cylinder surface, thus the characteristics of the flow field can be easily obtained. But the shear stress on the cable-surface cannot be obtained by measuring pressure on the surface(Han *et al.* 2016). The aerostatic coefficients at some inclination angles would be inaccurate due to the axial flow along the cylinder. Some researchers use the piezoelectric balance to measure the aerostatic coefficients of the circular cylinder(Schewe 1983, Xu *et al*. 2006, Poulin and Larsen 2007, Kleissl and Georgakis 2012, Matteoni and Georgakis 2012, Hoang *et al*. 2015). However, these tests were carried out in different wind tunnels where the quality of the flow field was different. Due to limitations of the test facility, the Reynolds number cannot reach the supercritical state and combinations of inclination angle and yawed angle are limited. In some research, the drag coefficient is emphasized while little attention is paid to the lift coefficient (Poulin and Larsen 2007). Therefore, there is no such a unified standard to evaluate the aerostatic coefficients. Current experimental results of aerostatic coefficients are limited in cable-wind angles and Reynolds number range. The aerodynamic characteristics of inclined and yawed smooth circular cylinders were investigated in a wide range of Reynolds number and orientation angles through numerical CFD simulation (Hoftyzer 2016). But few comprehensive experiment results could be found for validation. And researches on circular cylinder with the surface of dimpled pattern and helical fillet by CFD approach were seldom reported.

To enrich the data of existing research, the drag and lift coefficients of circular cylinders with

three surfaces were tested in a wide range of Reynolds numbers, with various combinations of inclined and yawed angles in this paper. From our test, the drag crisis occurs only in the critical state for the smooth surface and lift coefficients exhibit two steep variations in the critical state for the smooth surface. Adopting the existed quasi-steady model, the aerodynamic damping for cylinders with different surfaces were evaluated and compared.

2. Wind tunnel test

2.1 Wind tunnel

These wind tunnel tests were conducted in a closed circuit low speed wind tunnel located in the China Aerodynamic Development and Research Center (CARDC). Its test section is 4 m in width and 3 m in height. The wind speed can be adjusted from 10 m/s to 90 m/s. During the test, the mean wind speed was increased from 16 m/s to 60 m/s with a step of 2 m/s, thus ensuring the supercritical Reynolds number to be reached for the model. The quality of the flow field is very stable and the turbulence of the empty wind tunnel on average is 0.14%.

2.2 Model description

A typical application of inclined circular cylinders adopted in engineering practice is stay cables on bridges. So a cable model at the scale 1:1 was manufactured to ensure the Reynolds number similarity between the model and the prototype. The model of the cable with smooth surface configuration was manufactured using stainless tube first and shrouded with the same HDPE material used on cable-stayed bridges. The diameters of smooth models were measured 100 times at different locations along the tube, reaching an average value of 158 mm (referring to the nominal diameter of the cable) and standard deviation (σ) of 0.32 mm. The length of action model was 1.8 m to ensure length to diameter ratio 11.39.Based on the smooth surface cable, a cable with dimpled surface and a cable with helical surface (shown in Fig. 1) was adopted in the wind tunnel test. For the cable surface with a dimpled configuration, the model was manufactured by stamping the dimpled pattern on the surface of a smooth cable (see Fig. 2).The helical fillet, which is made by cutting a commercial PE plate into fillets, is 2 mm wide with a step 0.9 m (see Fig. 3).

2.3 Test facilities

To avoid the influence of end effects on the test results, two same pseudo models with a length at least 0.75 m depending on the inclination angles were installed at each end of the 1.8m long action model. The action model was fixed to the sting covered by pseudo model with the same surface, diameter and material as the action model at one end through one force balance. The balance was fixed inside the action model to render end effects unimportant. The pseudo model stings were connected to upper and lower model stings (shown in Fig. 6). Six pairs of stings which varied in length were prepared to provide the inclination angles from 20° to 60° with an increment of 10°. All stings were made of type 45 steel and they were fixed on two turntables on the top and bottom of the wind tunnel to facilitate the cable yaw to the wind.

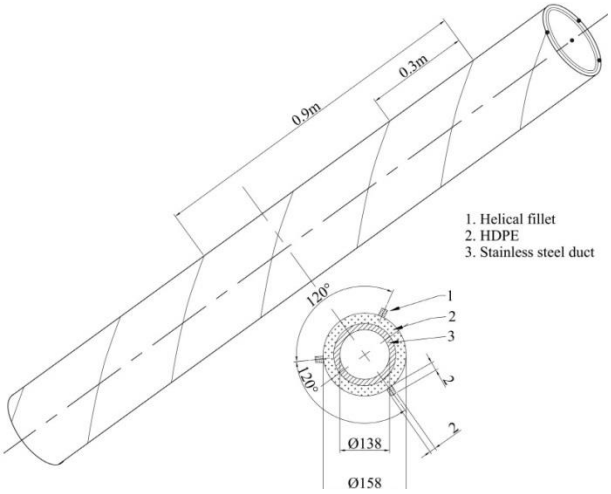

Fig. 1 Sketch of the cable tube

Fig. 2 Cable model with dimpled pattern on the surface

Fig. 3 Cable model with 2 mm helical fillet on the surface

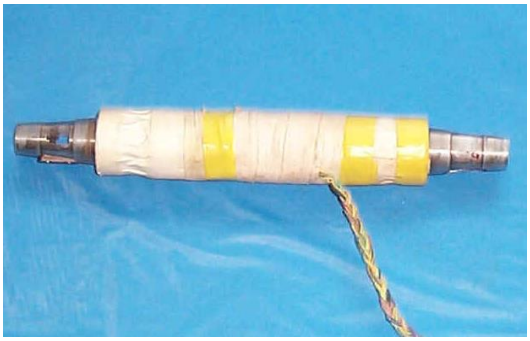

Fig. 4 TG0401 balance used for measuring the wind force acting on the circular cylinder

Fig. 5 Installation of the model system in the wind tunnel

It was estimated that the wind force on the model was in the range of 50N-350N varying with wind speeds and inclined and yawed angles. The total mass of the action model, connection parts, and the balance was estimated to be 20 kg. Thus, the balance of the type TG0401, which is a standard product of CARDC(Liang *et al*. 2007) containing 6 components (F_X,F_Y,F_Z,M_X,M_Y,M_Z) was chosen to measure the wind force, see Fig.4. Prior to commencement of actual test for the cable model with different surface configuration, the force balance was checked by exerting a system of loads along directions of drag, lift, and side forces. As the natural frequency of model system was 6-7 Hz, the possible resonance at a wind speed higher than 10 m/s due to vortex shedding was definitely avoided. As the frequency of vortex shedding may be up to 120 Hz, the sampling frequency will be set at 1000 Hz for a sampling time of 30 seconds.

2.4 Cable geometry

When the testing model and balance were installed properly in the wind tunnel, the whole system could be seen in Fig. 5. Moreover, Fig. 6 is a schematic diagram for the testing model, which exhibits the geometry of the cable in the wind tunnel.

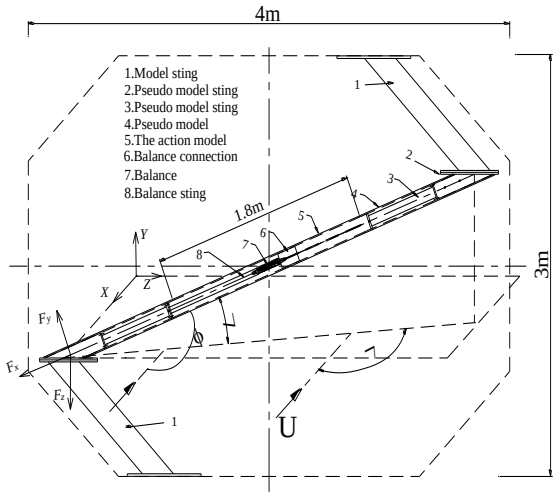

Fig. 6 Schematic diagram of the testing model in the wind tunnel

As shown in Fig. 6, α is defined as the inclination angle, which is angle between the cable and the wind tunnel floor. β is defined as the yaw angle, which indicates the angle between oncoming wind and the cable plane.

The wind force acting on the cylinder is measured using balance in the body coordinate system. To facilitate the follow-up calculation and analysis, wind forces can be transformed into the wind coordinate system. Let us consider the orthogonal wind coordinate system O-XYZ defined orienting X along the wind direction, and Y vertically directed upwards. For the body coordinate system o-xyz, each axis is parallel to the wind coordinate axis as shown in Fig. 6. When the cylinder is inclined or yawed, the body coordinate system rotates the corresponding same value of angle.

When generating a 3D rotation, the axis of rotation and amount of rotation should be specified. Then the rotated vector can be obtained by multiplying the rotation matrix. For example, when a vector $\boldsymbol{p}$= (a, b, c) rotates counter-clock wisely about the z-axis with an angle of θ, then the rotated vector $\boldsymbol{p'}$= (a', b', c') can be obtained as follows

$$\boldsymbol{p}' = \boldsymbol{R}_z(\theta)p \tag{1}$$

Where

$$\boldsymbol{R}_z(\theta) = \begin{bmatrix} cos\theta & -sin\theta & 0 \\ sin\theta & cos\theta & 0 \\ 0 & 0 & 1 \end{bmatrix} \tag{2}$$

When the vector p rotates counter clock-wisely about the x-axis or the y-axis with an angle of the corresponding rotation matrix R_x and R_y are expressed as follows

$$R_x(\theta) = \begin{bmatrix} 1 & 0 & 0 \\ 0 & cos\theta & -sin\theta \\ 0 & sin\theta & cos\theta \end{bmatrix} \tag{3}$$

$$\boldsymbol{R}_y(\theta) = \begin{bmatrix} cos\theta & 0 & sin\theta \\ 0 & 1 & 0 \\ -sin\theta & 0 & cos\theta \end{bmatrix} \tag{4}$$

Given the inclined and yawed angle of the cylinder α and β two rotations about the Y and Z axis would make the body coordinate system consistent with the wind coordinate system.

To transform the value in the body coordinate system to the wind coordinate system, the following composite rotations can be adopted.

$$\boldsymbol{F}_w = \boldsymbol{R}_y(-\alpha)\boldsymbol{R}_z(-\beta)\boldsymbol{F}_b \tag{5}$$

Where

$$\boldsymbol{F}_w = (F_X, F_Y, F_Z) \tag{6}$$

$$\boldsymbol{F}_b = (F_x, F_y, F_z) \tag{7}$$

Thus the drag force F_X and lift force F_Y in the wind coordinate system are derived using mean values of the force time history measured in the body coordinate system. The drag and lift coefficient (C_D and C_L) is defined in Eqs. (8) and (9).

$$C_D = \frac{F_X}{\frac{1}{2}\rho U^2 DL} \tag{8}$$

$$C_L = \frac{F_Y}{\frac{1}{2}\rho U^2 DL} \tag{9}$$

Where, ρ is the air density, U is the oncoming wind speed, D is the diameter of the cable and L is the length of the action model.

2.5 Reynolds number correction

The Reynolds Number is defined as $Re=UD/\nu$, where ν is the kinematical viscosity depending on wind tunnel temperature, U is the inflow velocity and D is the diameter of the circular cylinder. The temperature was 17.5℃ during the test. Thus the kinematic viscosity of the air ν is about 1.48×10^{-5} m^2/s (Schetz and Fuhs 1996). Due to the existence of turbulence in the wind tunnel, these Reynolds Numbers above are nominal. In fact, the drag coefficient is a function of effective Reynolds Number, which is the product of nominal Reynolds Number and factors decided by turbulence intensity, roughness etc. The quality of the flow field in CARDC 3×4 m wind tunnel is very stable, and the average turbulence intensity of the empty wind tunnel is 0.14%. So that the turbulence factor of the wind tunnel is found to be 1.13 from the known curve (Barlow *et al.* 1999).

The other factors related to roughness and oscillation, for the present investigations, was assumed to be 1. Thus the effective Reynolds number given in this paper is

$$Re_e = 1.13\frac{UD}{\nu} \tag{10}$$

The blockage ratio of the model in cross flow is lower than 3%. Thus, corrections about the drag and lift coefficients could be neglected according to Maskell III method(Hackett and Cooper 2001).

Table 1 Testing scheme for the cable in wind tunnel test

Cable surface	Yaw angle(°)	Inclination angle（°）
Smooth	0,10,10,90,170,180	20,30,40,50,60
Dimpled pattern	0,10,10,90,170,180	20,30,40,50,60
Helical fillet	0,10,10,90,170,180	20,30,40,50,60

2.6 Testing scheme

Considering the application of inclined circular cylinder in engineering practice, 5 typical inclination angles and 5 yaw angles have been chosen for the cable with 3 different surfaces (i.e., smooth, dimpled pattern and helical fillet) in the wind tunnel test. The detailed test scheme is shown in Table 1.

Because the "dirt", such as the fingerprint or ash, accumulated on the surface of the cylinder would change the surface roughness thus influencing the flow transitions, so the cylinder was cleaned carefully every time after each test case finished.

3. Results and discussions

3.1 Verification of test accuracy

To check the accuracy of test results, a series of repeating tests were conducted. Fig. 7 shows the results of 5 tests for the smooth surface model at α= 60° and β = 90°. The standard deviation (σ) of drag coefficients was calculated by using those data. When wind speed was below 20 m/s, the maximum deviation (3σ) was then found to be ±0.04. When wind speed was over 24 m/s, the maximum deviation was found to be ±0.01, which is consistent with the accuracy of the balance type TG0401.And it should be noticed that in Fig. 7 and relevant results after mentioned, the Reynolds number is the one corrected considering the effects of turbulence.

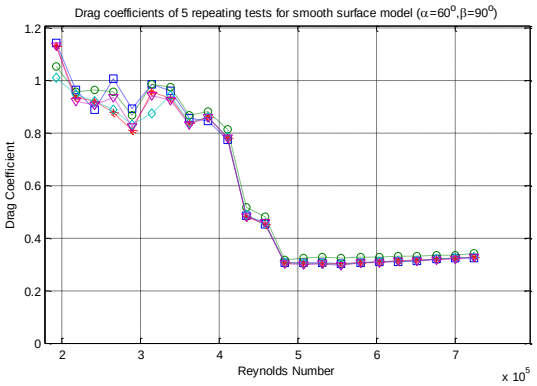

Fig. 7 Drag coefficients of 5 repeating tests

3.2 Effects of inclination angle

The commonly used circular cylinders in various structures may have different inclination angles. Because the adoption of surface configuration with helical fillet or dimpled pattern would change the characteristics of flow around the circular cylinders significantly, only the smooth circular cylinder is selected to investigate the effects of inclination and yawed angle on drag/lift coefficients for the brevity of research.

From Fig. 8, it can be found that the drag coefficient is insensitive to the inclined angle when the yaw angle is 90°. When the circular cylinder is yaw to the wind, the drag coefficient would increase with the inclined angle. When the yaw angle is 90°, the maximum value of drag coefficient would reach approximately 1.2, while the maximum value would drop to 0.8 when the circular cylinder is yawed to wind at different inclination angles. The drag crisis can be seen in several inclined angles, which is an indication of the occurrence of the critical state.

With the initiation of the critical state, the drop of drag coefficients is accompanied by the sudden change of lift coefficients. Referring to other studies, the sudden change of lift appears at large yaw angles. The consistent result can be found in this test when the yaw angle is 90°. The maximum value of lift coefficient changes with the variation of the inclination angle. The lift coefficients are always positive in this test except that when α=60°, the sign of the lift coefficient changes to negative. It is addressed that the surface roughness would change the lift coefficients significantly(Matteoni and Georgakis 2012).

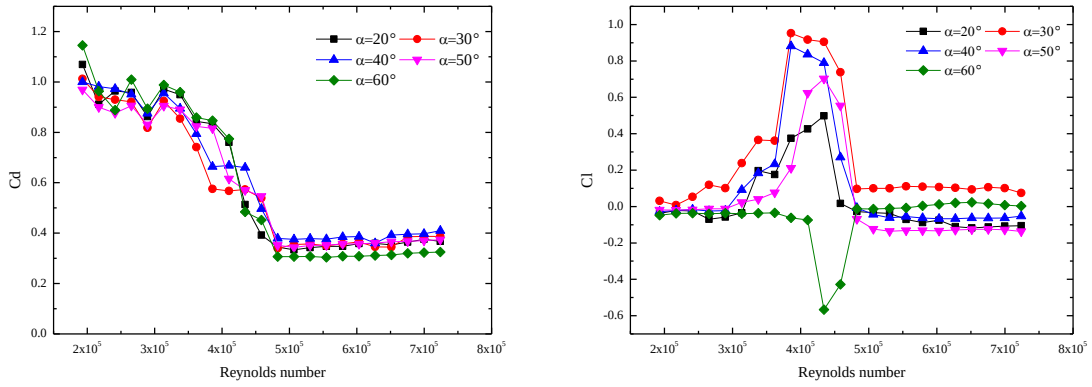

(a) β=90°

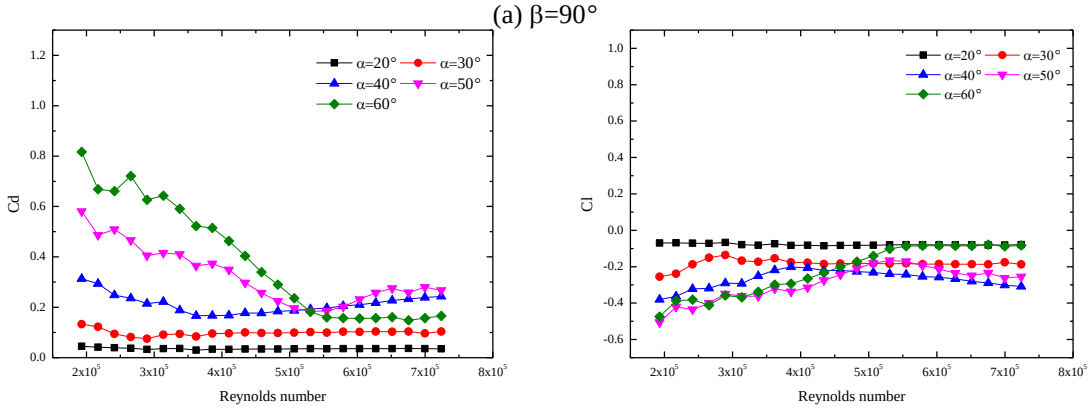

(b) β=0°

Continued-

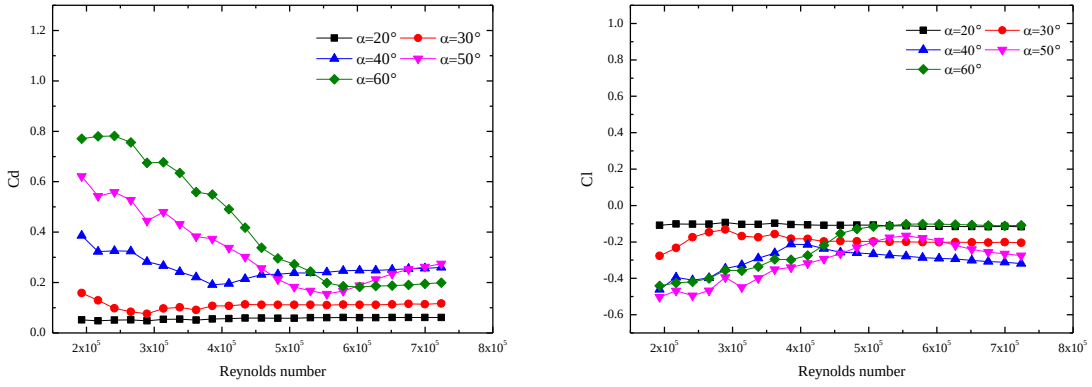

(c) β=10°

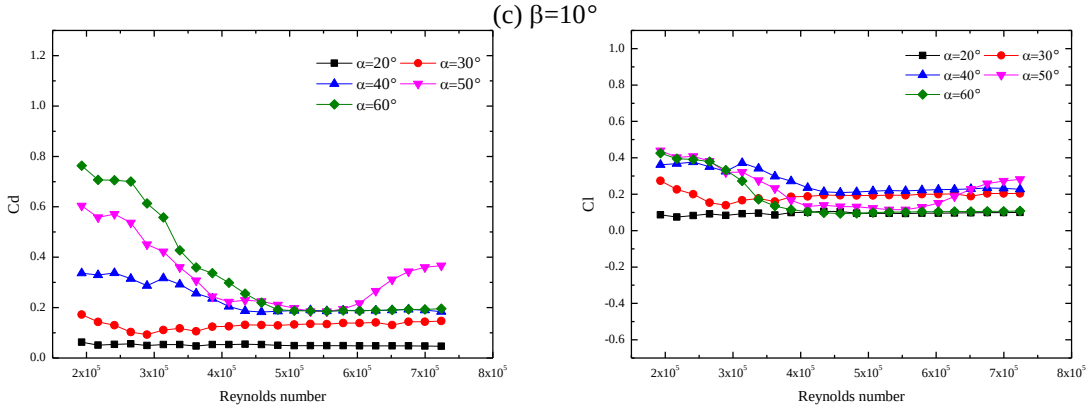

(d) β=170°

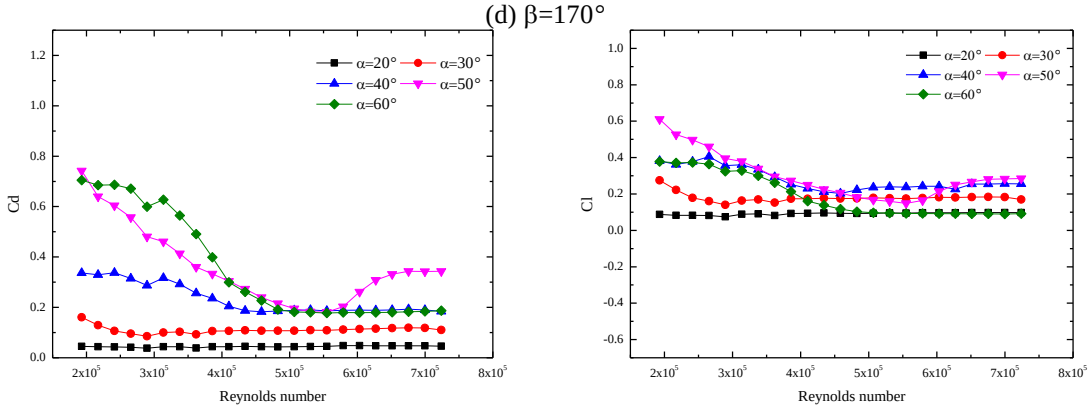

(e) β=180°

Fig. 8 Drag and lift coefficients under different inclination angles

However, the smooth circular cylinder with the same yaw angle, which means the same surface exposed to the wind, exhibits large variations of lift coefficients with different inclined angles.

The sign was considered to be determined by the position of the initial separation of the bubble (Macdonald and Larose 2006). Despite the sign of the lift coefficients, the value of the lift coefficient was closely related to the inclination angle. Therefore, it can be conjectured that a complex axial flow pattern exists along the cylinder, though there is not much evidence in flow

visualization. When the yaw angle is not 90°, the lift coefficient would decrease as the increment of Reynolds number obviously in the critical state. In the supercritical state, the lift coefficient is close to zero with little variation. For the inclination angle of 20°, the lift coefficient experiences little variation with the Reynolds number and was close to zero.

3.3 Effects of yaw angle

Only the circular cylinder with the smooth surface is considered here as the previous section.

From Fig. 9, it can be observed that the yaw angle plays a significant role in the drag coefficients. The drag crisis appears only when β=90° and the drag coefficients would reach its maximum value at each inclination angle. The influence of yaw angle on drag coefficients decreases with the increment of inclination angle. The drag coefficients reach more consistent value at different yaw angles when α=50° and 60°. At other inclination angles, the drag is very different between the case of β=90° and other yaw angles.

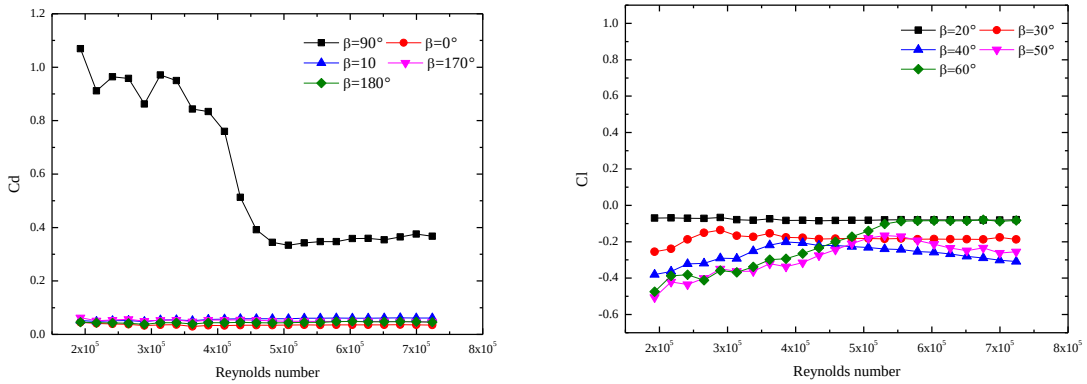

(a) α=20°

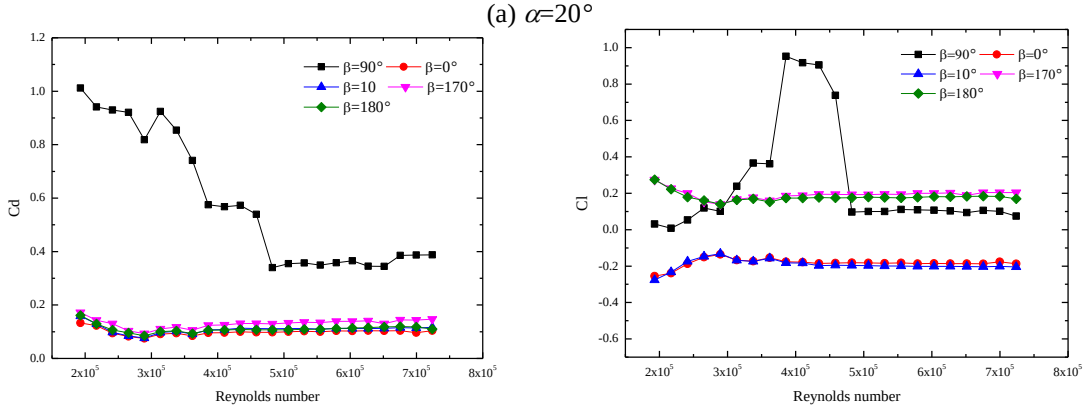

(b) α=30°

Continued-

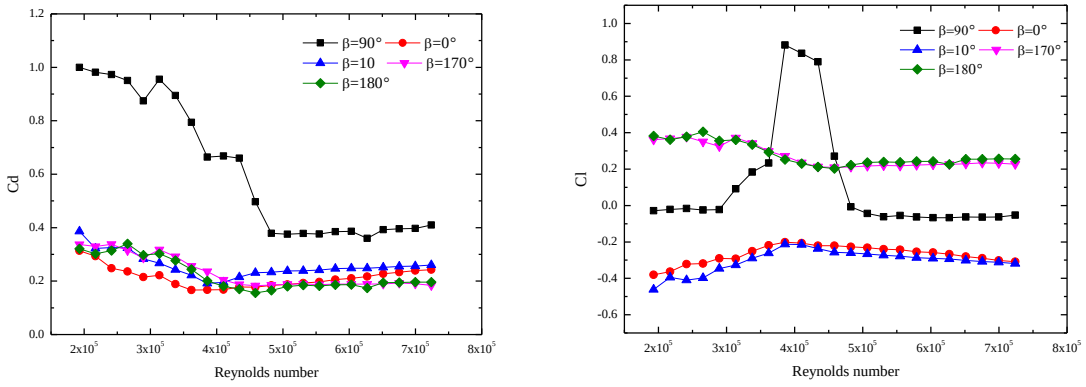

(c) α=40°

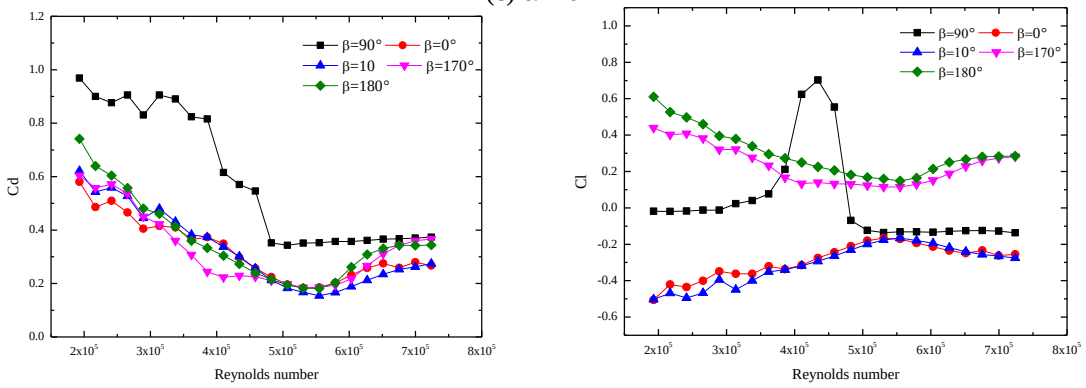

(d) α=50°

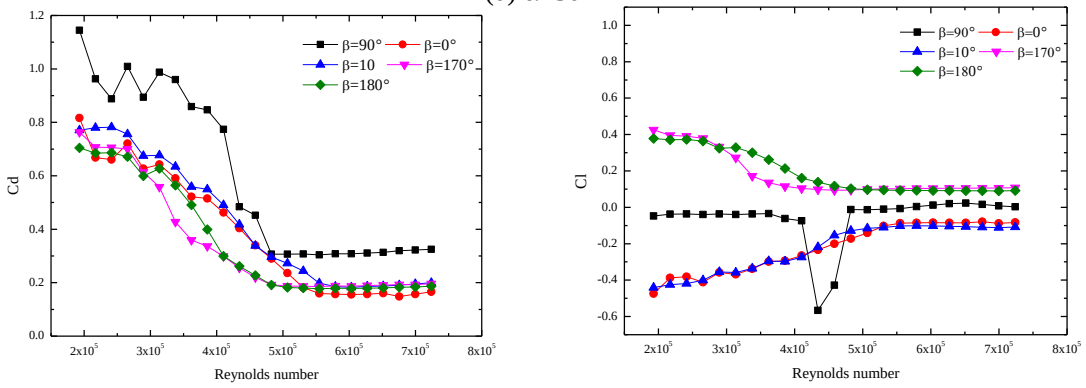

(e) α=60°

Fig. 9 Drag and lift coefficients under different yaw angles

In terms of the lift coefficients, the abrupt change in the critical Reynolds number state only occurs when β =90°. For other yaw angles, the lift coefficient for β =0°,10° and β =180°, 170° are opposite to each other, with the previous ones showing the positive value and the latter one showing the negative value. According to existed research, it suggests that non-identical distribution of surface roughness would result in the separation position of the bubble and influence the sign of the lift coefficient. When β =90°, the steady lift only occurs in critical state and randomness exists in

the sign of the lift coefficient. The inherent mechanism of this phenomenon needs further research to be clarified.

3.4 Effects of surface configuration

In terms of the influence of surface configurations, the circular cylinder with dimpled pattern surface and helical fillet are tested in the wind tunnel. The same with the smooth circular cylinder, the testing cases include several combinations of inclination and yaw angles. From the results summarized in 3.2 and 3.3, the yaw angle of 90° and the inclination angle of 20° and 60° are chosen for comparison. The drag and lift coefficients are shown in Figs. 10 and 11.

It is observed that the drag coefficients can be reduced effectively in the sub-critical and critical state by adopting the dimpled pattern surface and helical fillet surface. The drag crisis disappears when the surface configuration of the cylinder changes. However, the drag coefficients for the cylinders with dimpled pattern surface and helical fillet were larger than the smooth one in the post-critical state.

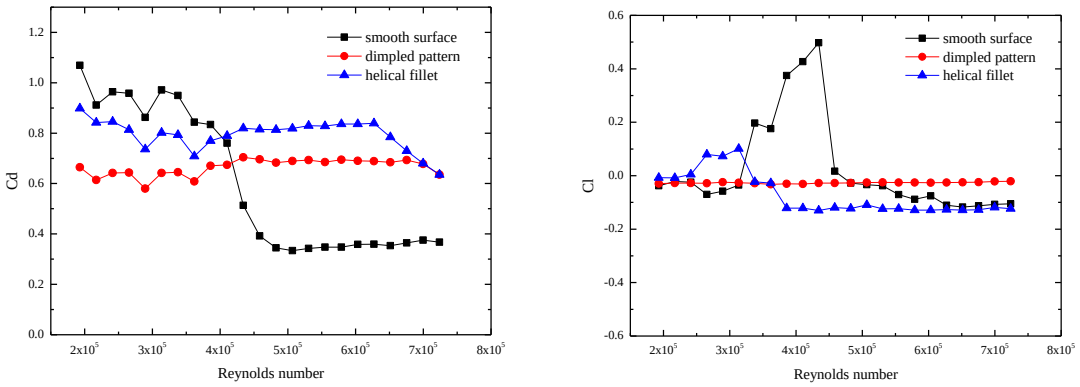

Fig. 10 Drag and lift coefficients for different surface configurations (α=20°, β=90°)

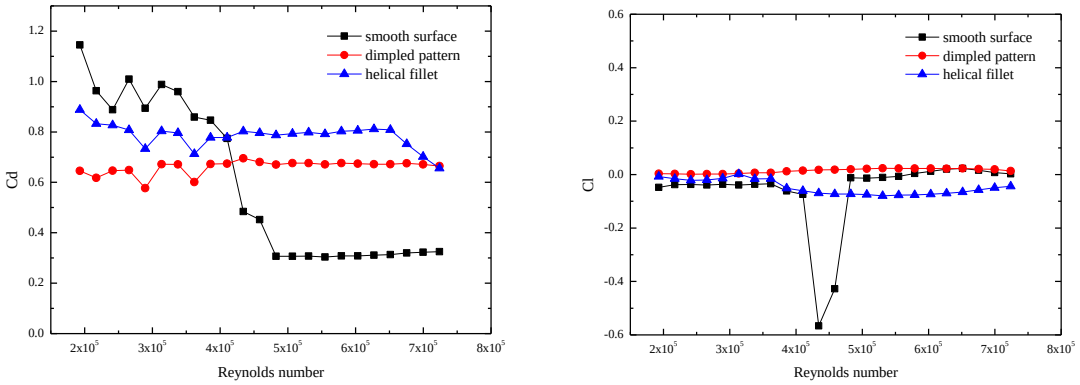

Fig. 11 Drag and lift coefficients for different surface configurations (α=60°, β=90°)

On the other hand, the adoption of dimpled pattern and helical fillet surface, the steady lift would not occur during the whole range of Reynolds number. The occurrence of the random sign for the lift coefficient also disappears regardless of the inclination angle. Considering the effects of inclination angle on the lift coefficients for the smooth circular cylinder, the different characteristics of lift for the dimpled pattern and helical fillet can be noticed as the change of the axial flow and the three-dimensional flow separation (Yagi *et al.* 2010). The dimpled pattern of helical fillet disturbs the flow along and around the cylinder, thus the steady lift would not appear in the critical state. The possible mechanisms are given and further experimental research should be carried out to decide their importance on influencing the aerodynamic coefficients of the cable in these cases.

3.5 Evaluation of nondimensional aerodynamic damping parameter

With the obtained aerodynamic coefficients, the aerodynamic damping of the circular cylinders can be evaluated based on the quasi-steady assumption (Macdonald and Larose 2006). The nondimensional aerodynamic damping parameter considering the Reynolds number, the angle between wind velocity and the cable axis, and the orientation of the vibration plane is defined in Eq. (11).

$$\begin{aligned} Z_a = -\frac{\mathrm{Re}}{8\pi}\cos\gamma\Bigg\{&\cos\gamma\left[C_D(2\sin\phi+\frac{\tan^2\gamma}{\sin\phi})+\frac{\partial C_D}{\partial \mathrm{Re}}\mathrm{Re}\sin\phi+\frac{\partial C_D}{\partial \mathrm{Re}}\cos\phi\right] \\ &-\sin\gamma\left[C_L(2\sin\phi-\frac{1}{\sin\phi})+\frac{\partial C_L}{\partial \mathrm{Re}}\mathrm{Re}\sin\phi+\frac{\partial C_L}{\partial\phi}\cos\phi\right]\Bigg\} \end{aligned} \tag{11}$$

Where *Re* is the Reynolds number, γ is the angle represents the orientation of the vibration plane, ϕ is the cable-wind angle, C_D is the drag coefficient and C_L is the lift coefficient.

In terms of the cable-wind angle, it can be calculated from Eq. (12).

$$cos\phi = cos\alpha cos\beta \tag{12}$$

Where ϕ is the cable-wind angle, α is the inclination angle and β is the yaw angle mentioned in section 2.4.

During the wind tunnel test, the combination of typical inclination and yaw angles yields a set of cable-wind angle ranges from 20° to 160°. However, different inclination angles will result in the same cable-wind angle when the yaw angle β=90°. Drag coefficients under different inclination angles show good consistency when β=90°. This trend applies to all three surface configurations for the circular cylinder. Due to the axial flow along the cylinder, the lift coefficients vary in both value and sign as the inclination angle changes, when the yaw angle is 90°. So five sets of drag coefficient at ϕ=90° were averaged for calculation while the lift coefficient for each inclination angle was treated separately.

To evaluate the nondimensional aerodynamic damping parameter based on Eq. (11), two-dimensional linear interpolations of drag and lift coefficient considering the Reynolds number and the cable-wind angle are done first, which are shown Figs. 12-14.

Referring to the existed test of the dynamic cable model, the angle γ=54.7° was the orientation when the divergent dry galloping occurs(Cheng *et al.* 2003). The corresponding full-scale cable inclination angle is 45°. So the lift coefficient of similar inclination angles (α=50°, β=90°) is chosen for the calculation. The contours of nondimensional aerodynamic damping parameter for three surface configurations are shown in Fig. 15. It can be seen that the minimum value of the

nondimensional aerodynamic damping parameter for the dimpled pattern is higher than the one with smooth surface or helical fillet. By replacing the lift coefficient with values from other inclination angles (i.e., 20°,30°,40°and 60°) when β=90°, the minimum nondimensional aerodynamic damping parameter for each case are listed in Table 2.

The same results come out when the lift coefficient (at β=90°) of other inclination angles were adopted. It can be concluded that the dimpled pattern surface is more effective measure to suppress dry galloping of cables compared with the helical fillet. Thus the dimpled pattern on the surface of the circular cylinder can be considered as a potential measure for suppressing dry galloping.

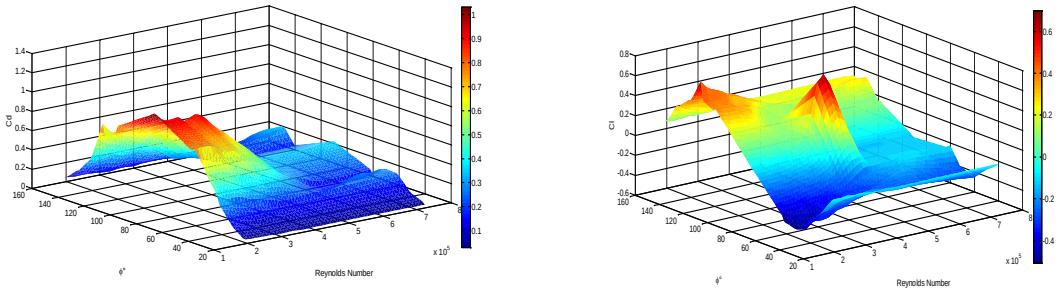

Fig. 12 Drag and lift coefficients for circular cylinder with smooth surface

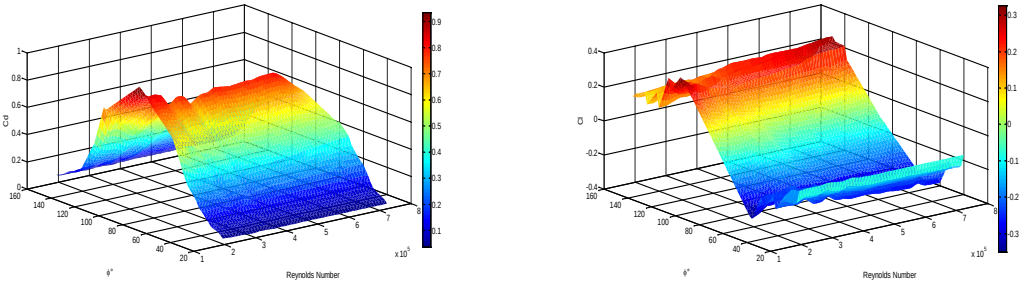

Fig. 13 Drag and lift coefficients for circular cylinder with helical fillet

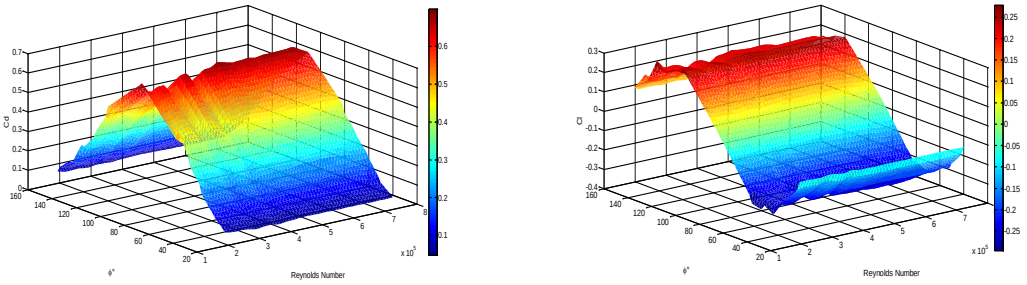

Fig. 14 Drag and lift coefficients for circular cylinder with dimpled pattern

Table 2 Minimum nondimensional aerodynamic damping parameter for each inclination angle selected

Inclination angle	Surface configuration		
	Smooth	Helical fillet	Dimpled pattern
20°	-1.68×10^{4}	-5.02×10^{3}	-4.53×10^{3}
30°	-6.55×10^{4}	-5.02×10^{3}	-4.53×10^{3}
40°	-7.16×10^{4}	-5.02×10^{3}	1.03×10^{3}
60°	-7.21×10^{4}	-5.02×10^{3}	1.03×10^{3}

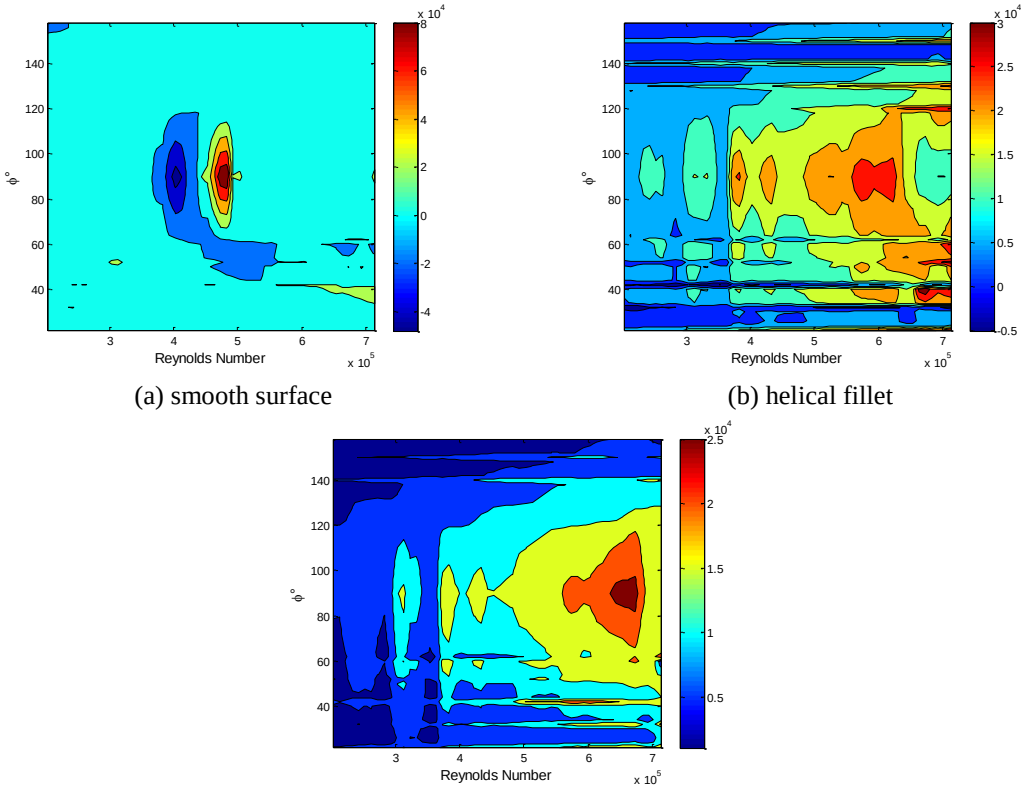

(a) smooth surface (b) helical fillet

(c) dimpled pattern

Fig. 15 Nondimensional aerodynamic damping parameter Z_a

4. Conclusions

By conducting a series of wind tunnel tests on the aerodynamic coefficients of inclined and yawed circular cylinders and evaluating the nondimensional aerodynamic damping parameters for three different circular cylinders, conclusions can be drawn as follows.

- Drag coefficient would increase with the increment of inclination angle except when the yaw angle is 90° for the smooth circular cylinder. The influence of yaw angle on the drag coefficient was large at low inclination angle and vice versa.

- The occurrence of steady lift in the critical state can be observed when the yaw angle is 90°. The sign of the lift coefficient is opposite for yaw angle of 0°,10° and 180°, 170°. Due to the existence of axial flow along the cylinder, the influence of inclination angle on the lift coefficient is rather complex.
- Adopting the surface of helical fillet, the occurrence of steady lift and the drag can be reduced effectively.
- By evaluating the nondimensional aerodynamic damping parameter, the helical fillet and dimpled pattern surface have the potential to suppress dry galloping while the latter measure turns out to be more effective.
- Aerodynamic coefficients under a wide range of Reynolds number for different yaw angles and inclination angles can provide a reference for the CFD research in this field.

Acknowledgments

The research described in this paper was financially supported by the National Natural Science Foundation under the grant number 51278433. The authors would also like to thank the staffs in China Aerodynamics Research and Development Centre for their support during the wind tunnel test.

References

Acampora, A., Macdonald, J.H.G., Georgakis, C.T. and Nikitas, N. (2014), "Identification of aeroelastic forces and static drag coefficients of a twin cable bridge stay from full-scale ambient vibration measurements", *J. Wind Eng. Ind. Aerod*., **124**, 90-98.

Barlow, J.B., William H. Rae, J. and Pope, A. (1999), Low-speed wind tunnel testing, John Wiley&Sons, Inc.

Boujard, O. and Grillaud, G. (2007), "Inclined stay-cable vibrations: confrontation of full-scale measurements and quasi-steady analysis of wind-tunnel tests", *Proceedings of the 12th International Conference on Wind Engineering*, Cairns, Australia.

Carassale, L., Freda, A. and Piccardo, G. (2005), "Aeroelastic forces on yawed circular cylinders: quasi-steady modeling and aerodynamic instability", *Wind Struct*., **8**(5), 373-388.

Cheng, S., Larose, G.L., Savage, M.G. and Tanaka, H. (2003), "Aerodynamic behaviour of an inclined circular cylinder", *Wind Struct*., **6**(3), 197-208.

Hackett, J.E. and Cooper, K.R. (2001), "Extensions to Maskell's theory for blockage effects on bluff bodies in a closed wind tunnel", *Aeronaut. J*., **105**(1050), 409-418.

Han, Y., Chen, H., Cai, C.S., Xu, G., Shen, L. and Hu, P. (2016), "Numerical analysis on the difference of drag force coefficients of bridge deck sections between the global force and pressure distribution methods", *J. Wind Eng. Ind. Aerod*., **159**, 65-79.

Hoang, M.C., Laneville, A. and Légeron, F. (2015), "Experimental study on aerodynamic coefficients of yawed cylinders", *J. Fluid. Struct*., **54**, 597-611.

Hoftyzer, M.S. (2016), Aerodynamic Characteristics of Yawed Inclined Circular Cylinders, Université d'Ottawa/University of Ottawa, Ottawa,Canada.

Jakobsen, J.B., Andersen, T.L., Macdonald, J.H.G., Nikitas, N., Larose, G.L., Savage, M.G. and McAuliffe, B.R. (2012), "Wind-induced response and excitation characteristics of an inclined cable model in the critical Reynolds number range", *J. Wind Eng. Ind. Aerod*., **110**, 100-112.

Jing, H., Xia, Y., Li, H., Xu, Y. and Li, Y. (2017), "Excitation mechanism of rain–wind induced cable

vibration in a wind tunnel", *J. Fluid. Struct*., **68**, 32-47.
Kleissl, K. and Georgakis, C.T. (2012), "Comparison of the aerodynamics of bridge cables with helical fillets and a pattern-indented surface", *J. Wind Eng. Ind. Aerod*., **104-106**, 166-175.
Larose, G., Savage, M. and Jakobsen, J. (2003), "Wind tunnel experiments on an inclined and yawed circular cylinder in the critical Reynolds number range", *Proceedings of the 11th International Conference on Wind Engineering*, Lubbock, Texas.
Liang, J., Zhang, W.G., Wang, X.N. and Du, J.H. (2007), "Development for restraining oscillation device of the UAV model in the 4 m× 3 m wind tunnel ", *J. Exp. Fluid Mech*., **4**, 014.
Macdonald, J.H.G. and Larose, G.L. (2006), "A unified approach to aerodynamic damping and drag/lift instabilities, and its application to dry inclined cable galloping", *J. Fluid. Struct*., **22**(2), 229-252.
Matsumoto, M., Yagi, T., Liu, Q., Oishi, T. and Adachi, Y. (2005), "Effects of axial flow and Karman vortex interference on dry-state galloping of inclined stay-cables", *Proceedings of the 6th International Symposium on Cable Dynamics*.
Matteoni, G. and Georgakis, C.T. (2012), "Effects of bridge cable surface roughness and cross-sectional distortion on aerodynamic force coefficients", *J. Wind Eng. Ind. Aerod*., **104-106**, 176-187.
Nikitas, N., Macdonald, J.H.G., Jakobsen, J.B. and Andersen, T.L. (2012), "Critical Reynolds number and galloping instabilities: experiments on circular cylinders", *Exp. Fluids*, **52**(5), 1295-1306.
Poulin, S. and Larsen, A. (2007), "Drag loading of circular cylinders inclined in the along-wind direction", *J. Wind Eng. Ind. Aerod*., **95**(9-11), 1350-1363.
Raeesi, A., Cheng, S. and Ting, D.S.K. (2016), "Application of a three-dimensional aeroelastic model to study the wind-induced response of bridge stay cables in unsteady wind conditions", *J. Sound Vib*., **375**, 217-236.
Schetz, J.A. and Fuhs, A.E. (1996), Handbook of fluid dynamics and fluid machinery, Wiley New York
Schewe, G. (1983), "On the force fluctuations acting on a circular cylinder in crossflow from subcritical up to transcritical Reynolds numbers", *J. Fluid Mech*., **133**, 265-285.
Xu, Y., Li, Y., Shum, K., Kwok, K., Kwok, K. and Hitchcock, P. (2006), "Aerodynamic coefficients of inclined circular cylinders with artificial rivulet in smooth flow", *Adv. Struct. Eng*., **9**(2), 265-278.
Yagi, T., Okamoto, K., Sakaki, I., Koroyasu, H., Liang, Z., Narita, S. and Shirato, H. (2010), "Drag force reduction and aerodynamic stabilization of stay cables by modifying surface configurations", *Proceedings of the national symposium on wind engineering*.

AD